Pergamon

Bioorganic & Medicinal Chemistry 7 (1999) 1339–1347

BIOORGANIC & MEDICINAL CHEMISTRY

Synthesis and Evaluation of Inhibitors of Transthyretin Amyloid Formation Based on the Non-steroidal Anti-inflammatory Drug, Flufenamic Acid

Paul W. Baures, Vibha B. Oza, Scott A. Peterson and Jeffery W. Kelly*

Department of Chemistry and The Skaggs Institute of Chemical Biology, The Scripps Research Institute, 10550 North Torrey Pines Road, MB12, La Jolla, CA 92037, USA

Received 2 November 1998; accepted 2 December 1998

Abstract—A light scattering-based amyloid fibril formation assay was employed to evaluate potential inhibitors of transthyretin (TTR) amyloid fibril formation in vitro. Twenty nine aromatic small molecules, some with homology to flufenamic acid (a known non-steroidal anti-inflammatory drug) were tested to identify important structural features for inhibitor efficacy. The results of these experiments and earlier data suggest that likely inhibitors will have aromatic-based structures with at least two aromatic rings. The ring or fused ring system occupying the outermost TTR binding pocket needs to be substituted with an acidic functional group (e.g. a carboxylic acid) to interact with complimentary charges in the TTR binding site. The promising TTR amyloid fibril inhibitors ranked in order of efficacy are: **2** > **4**≈**7** > **3** > **9** > **6** > **21** (see Fig. 5).

Introduction

One of the common features of human amyloid disease is the deposition of insoluble high molecular weight cross-β-sheet fibrils derived from the self-assembly of one of 20 human proteins.[1–7] In the case of transthyretin (TTR), the process of amyloid fibril formation appears to be the causative agent in senile systemic amyloidosis (SSA) and familial amyloid polyneuropathy (FAP).[7,8] Wild-type TTR can be transformed into amyloid by partial denaturation (e.g. at reduced pH), affording a monomeric amyloidogenic intermediate with an alternatively folded structure that self-assembles into amyloid fibrils.[1–3,9–15] Transthyretin is a stable tetramer under physiological conditions; however, a low pH environment such as that encountered in an endosome or lysosome (or an analogous non-acidic denaturing environment) dissociates TTR into monomeric subunits as well as facilitating a conformational change within the TTR monomer making it amyloidogenic.[16] The >50 mutations associated with FAP make the kinetics and thermodynamics of this process more facile.[12–14,17]

Transthyretin normally binds to the thyroid hormone thyroxine (**1**, T_4) with negative cooperativity and high affinity (K_{A1} 10^8; K_{A2} 10^6), serving as the primary carrier of T_4 in the cerebral spinal fluid (CSF). However in plasma, TTR serves as the backup carrier for T_4, thyroid binding globulin being the primary carrier (K_A 6×10^9). Our strategy for inhibiting transthyretin amyloid fibril formation is to identify a ligand that will bind to TTR in human plasma using the largely unoccupied (≈90% unoccupied) T_4 binding site. Ligand binding stabilizes transthyretin and as a result also increases the activation barrier associated with the tetramer to monomeric amyloidogenic intermediate transition, i.e. the enabling event in amyloid fibril formation.[18] Previous results from our laboratory demonstrate that thyroxine is capable of stabilizing the tetrameric form of transthyretin, preventing amyloid fibril formation at a pH below 5.5 where TTR normally self-associates into amyloid fibrils.[15] Thyroid hormone also appears to stabilize TTR in the CSF in vivo, preventing fibril formation. Numerous pathological evaluations suggest that TTR amyloid fibrils are generally not observed in the brain.[15] This is the case even when a particularly unstable and pathogenic FAP variant such as L55P is expressed in the CSF, consistent with the role of T_4 as a TTR stabilizing agent in the CSF.

The stagnant fibril formation assay developed by our laboratory[11,15] was used to discover the non-steroidal anti-inflammatory drug flufenamic acid (Flu, **2**), which is an excellent TTR fibril inhibitor.[19] Flufenamic acid binds with high affinity and negative cooperativity (pH 7.6) to wild-type ($K_{D1} = 30 \pm 14$ nM, $K_{D2} = 255 \pm 97$ nM), V30M ($K_{D1} = 41 \pm 10$ nM, $K_{D2} = 320 \pm 125$ nM)

Key words: Transthyretin; amyloid fibril; inhibition; screening; NSAID.

* Corresponding author. Tel.: 858-784-9605; fax: 858-784-9610; e-mail: jkelly@scripps.edu

0968-0896/99/$ - see front matter
PII: S0968-0896(99)00066-8

and L55P TTR ($K_{D1} = 74 \pm 16$ nM, $K_{D2} = 682 \pm 137$ nM), completely inhibiting amyloid fibril formation at a concentration of 10.8 μM, 3× the physiological concentration of TTR (3.6 μM), under conditions where TTR amyloid fibril formation is maximal (pH 4.4).[19] A cocrystal structure of TTR with flufenamic acid was determined to 2.0 Å resolution in collaboration with the Sacchettini laboratory.[19] This structural information provides the basis for a rational drug design effort centered on identifying the important pharmacophoric substructures of flufenamic acid, such that subsequent parallel syntheses could be utilized to make an optimized ligand.

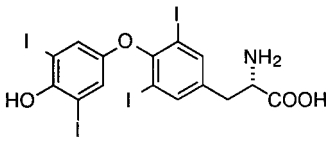

1, Thyroxine (T_4)

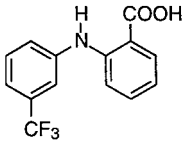

2, Flufenamic Acid

The compounds synthesized and reported in this paper were designed to test the important structural features of flufenamic acid that render it a good inhibitor (Fig. 1). Each of the five molecular fragments of Flu (fragments A–E) were evaluated in the structure–activity analysis described herein to differing extents. Such information should eventually lead to a generalizable pharmacophore hypothesis and help identify other novel ligands as represented by the generic structure on the right side of Figure 1. In this paper we report fibril inhibition data for several NSAIDs including flufenamic acid analogues utilizing the proven stagnant amyloid fibril formation assay.[11,15,18] The data suggests that the carboxylic acid functionality plays an important role in the binding of amyloid fibril inhibitors to TTR. In addition, there are also clear preferences for the aromatic platform that is capable of making van der Waals interactions with the TTR binding site.

Results

The structures of compounds either purchased or prepared for this study are shown in Figures 2 and 3. The NSAIDs diclofenamic acid (**3**), niflumic acid (**4**), indomethacin (**5**), sulindac (**6**), diflunisal (**7**), and tolmetin (**8**) (Fig. 2), as well as *N*-phenylanthranilic acid (**9**),

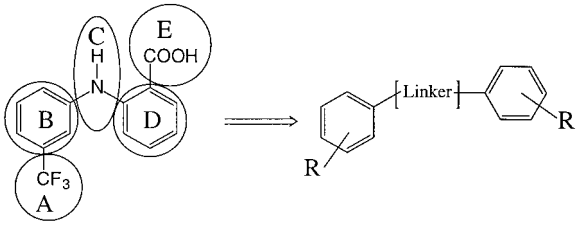

Figure 1. Flufenamic acid is logically divided into substructures labeled A–E to identify the portions of the Flu molecule that are essential for TTR fibril inhibition. This exercise was performed to identify the appropriate linker atom or group, R groups and the appropriate aromatic substructure for an optimal TTR fibril inhibitor.

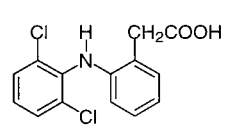

3, Diclofenamic Acid

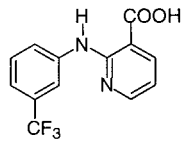

4, Niflumic Acid

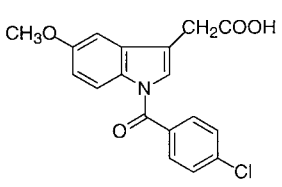

5, Indomethacin

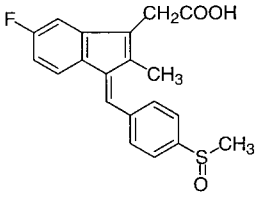

6, Sulindac

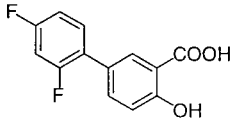

7, Diflunisal

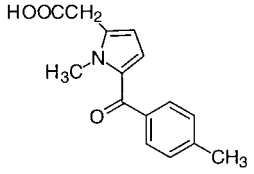

8, Tolmetin

Figure 2. Structural representation of the non-steroidal antiinflammatory drugs evaluated as possible inhibitors of transthyretin amyloid fibril formation.

meta-trifluoromethylaniline (**10**), and *para*-aminobenzoic acid (**12**) (Fig. 3) were all purchased and used without further purification. *N*-Acetyl-*meta*-trifluoromethylaniline (**11**) was prepared by acylation of **10** with acetic anhydride in pyridine Fig. (3). Compounds **13–15** (Fig. 3) were prepared by reductive amination of the imine formed by reaction of the appropriate aniline and benzaldehyde.[20] Addition of the appropriate aminobenzoic acid and trifluoromethyl-phenylisocyanate in THF yielded the urea linked compounds **16–24**, whereas compounds **25–27** were prepared by treating the appropriate aminobenzoic acid with phenylisocyanate.[21] The addition of *meta*-trifluoromethylbenzoyl chloride to either *meta*- or *para*-aminobenzoic acid affords the benzamides **28** and **29**, respectively.

The potential inhibitors shown in Figures 2 and 3 were evaluated in a 72 h stagnant fibril formation assay described previously.[11,15] Briefly, this assay subjects TTR (3.6 μM) to acidic partial denaturation at pH 4.4 (acetate buffer, 37 °C) in either the absence (assigned to be 100% fibril conversion) or in the presence of a potential amyloid fibril inhibitor. The extent of fibril inhibition is determined by the optical density measured on a UV spectrophotometer either at 330 or 400 nM in the presence of inhibitor relative to the OD reading in the absence of inhibitor (400 nM monitoring is employed for drug candidates that absorb significantly at 330 nM).[11,15] A quantitative congo red binding assay is also performed on promising inhibitors to confirm the

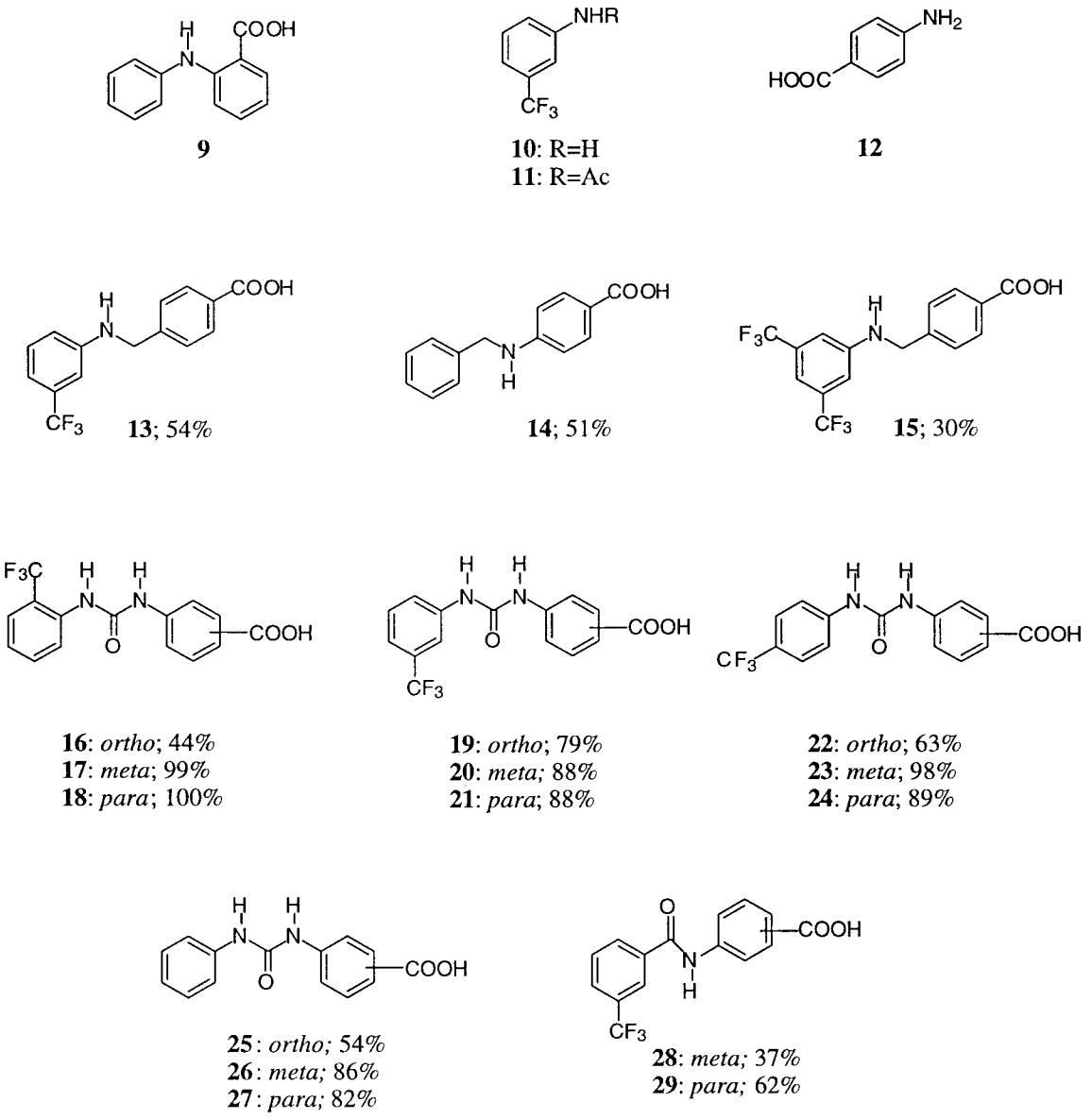

Figure 3. Structural representation of the aromatic compounds evaluated as possible inhibitors of transthyretin amyloid fibril formation. Compounds having yields associated with the compound number were synthesized by our laboratory, the remainder were procured from commercial sources.

light scattering results, which have proven to be extremely reliable. All potential inhibitors were tested initially at 36 μM, 10× the physiological TTR concentration (3.6 μM), to determine whether there was sufficient activity to warrant further assessment. When comparing inhibitors it is important to remember that the percent conversion of soluble transthyretin into fibrils over a 72 h period relative to transthyretin fibril conversion in the absence of inhibitor is reported. Hence, 100% fibril conversion (fibril formation) reflects no inhibition, whereas 0% conversion is complete inhibition of TTR fibril formation. We also carried out flufenamic acid (10.8 μM) inhibition of TTR fibril formation in each experiment to calibrate the new inhibitor results (see next paragraph).

The exact amount of TTR amyloid fibril formation observed from assay to assay is affected by the purity and age of the TTR sample used. In general, the preliminary evaluation of potential inhibitors carried out at a concentration of 36 μM was done with TTR (3.6 μM) estimated to be between 90 to 95% pure (SDS-PAGE analysis). None of these assays were done with TTR less than 90% pure. In experiments with older TTR (>1 month of age) or protein with ≈10% impurities present or both, we occasionally observed up to a 5% increase in the extent of apparent amyloid fibril formation. The largest contribution to the apparent increase in fibril formation (light scattering) in the less pure samples results from protein impurities that also self-assemble under amyloid forming conditions, leading to a higher OD reading at 400 nM. We always employ Flu (**2**) (10.8 μM) for the known inhibitor control in our preliminary screening experiments to get a handle on TTR batch to batch variability. The extent of conversion of soluble TTR (>90% pure) to amyloid fibrils in the

presence of 10.8 μM Flu was typically less than 5%. The range of 1–5% fibril conversion for Flu inhibition results from additional light scattering caused by impurities aggregating. We always re-evaluate encouraging results using >95% purity TTR, which typically yields only 1% conversion of TTR to fibrils in the presence of 10.8 μM Flu (Table 2).

The evaluation of potential inhibitors employing the fibril formation assay is summarized in Table 1. With the exception of sulindac (**6**) and tolmetin (**8**), the NSAIDs shown in Figure 2 were generally very good inhibitors, keeping fibril conversion to less than 5% of the control (100%) when evaluated at a concentration of 36 μM (10× [TTR]). Sulindac (**6**) was a good inhibitor, allowing only 14% conversion of TTR to fibrils relative to the positive control, whereas tolmetin is a poor inhibitor exhibiting conversion of 75% of TTR into amyloid fibrils. The remaining compounds shown in Figure 3 were generally less effective, with the exception of *N*-phenylanthranilic acid (**9**) and *N*-benzyl-*para*-aminobenzoic acid (**14**) which allowed only 2 and 6% conversion into amyloid fibrils, respectively (36 μM). Compounds **13**, **16**, **17** and **21** (Fig. 3) were modest inhibitors, holding amyloid fibril conversion to less than 25% of that observed in the positive control at an inhibitor concentration of 36 μM.

Compounds **3**, **4**, **6**, **7**, **9**, and **21** were evaluated in triplicate using highly purified wild-type TTR at inhibitor concentrations of 10.8 μM (3×[TTR]), 3.6 μM (1×[TTR]) and 1.8 μM (0.5×[TTR]), facilitating a direct comparison to the established inhibitor flufenamic acid, **2**.[18,19] In addition to light scattering, the extent of amyloid fibril formation was also evaluated using a quantitative congo red binding analysis, congo red being a dye that exhibits selective binding to amyloid fibrils.[22] The results of this assay are summarized in Table 2 and illustrated in bar graph format in Figure 4. Flufenamic acid (**2**) at a concentration of 10.8 μM, or 3× the TTR concentration, is capable of keeping fibril formation to less than 1% of that observed in the positive control. The fibril conversion yield increases to 26% and 57% as the concentration of flufenamic acid is reduced to 3.6 μM and 1.8 μM, respectively. Diclofenamic acid (**3**), niflumic acid (**4**), and *N*-phenylanthranilic acid (**9**) have the greatest homology to **2**. NSAID **4** is nearly as good as Flu (**2**) as an amyloid fibril inhibitor. The NSAIDs **3** and **9** exhibit a bit less than a two fold drop in activity relative to Flu at an inhibitor concentration of 3.6 μM. Sulindac (**6**) and **21** were not nearly as effective at these concentrations.

Of the NSAIDs that are not of the anthranilic acid class, diflunisal (**7**) gave the best results. Diflunisal is a very promising compound, and the biphenyl substructure an appealing platform to develop a new class of TTR amyloid fibril inhibitors. At a concentration of 10.8 μM, inhibitor **7** is indistinguishable from inhibitors **2** and **4**, all three exhibiting less than 1% conversion to amyloid fibrils. At an equal inhibitor to protein concentration ratio (3.6 μM) **7** is very similar to **2** and **4**, affording 35%, 26% and 32% fibril formation conversion yields, respectively. The promising inhibitors tested at a concentration of 3.6 μM ranked in order of efficacy are: **2** > **4**≈**7** > **3** > **9** > **6** > **21** (Fig. 5). This order of effectiveness is also maintained at an inhibitor concentration of 1.8 μM. The congo red results, which report on the extent of TTR fibril formation as a function of inhibitor concentration parallel the results derived from light scattering at 400 nM (Fig. 4). Negative values are sometimes observed in the congo red binding analysis when fibril formation is minimal, such as the case for inhibitors **2**, **3**, **4**, **7** and **9** when evaluated at a concentration

Table 1. Amyloid fibril inhibition by the compounds shown in Figure 1[a]

Compound	Percent fibril formation[b]
3	3
4	2
5	3
6	14
7	3
8	74
9	2
10	100
11	100
12	100
13	15
14	6
15	36
16	22
17	18
18	39
19	35
20	52
21	20
22	100
23	75
24	50
25	55
26	81
27	57
28	83
29	86

[a] The TTR concentration was 3.6 μM and the compounds were evaluated at 36 μM.
[b] Control fibril formation was determined in each assay in the absence of drug and was assigned to be 100%.

Table 2. Amyloid fibril inhibition with selected compounds at varying concentrations[a]

	Concentration (μM)		
	10.8	3.6	1.8
Compound	Percent fibril formation[b]		
2	1	26	57
3	2	47	69
4	1	32	62
6	19	67	80
7	1	35	66
9	5	51	72
21	59	86	91

[a] The TTR concentration was 3.6 μM and the NSAIDs were evaluated at 10.8 μM, 3.6 μM and 1.8 μM (3, 1 and 0.5 × the TTR concentration, respectively).
[b] Control fibril formation was determined in each assay in the absence of drug and was considered to be 100%.

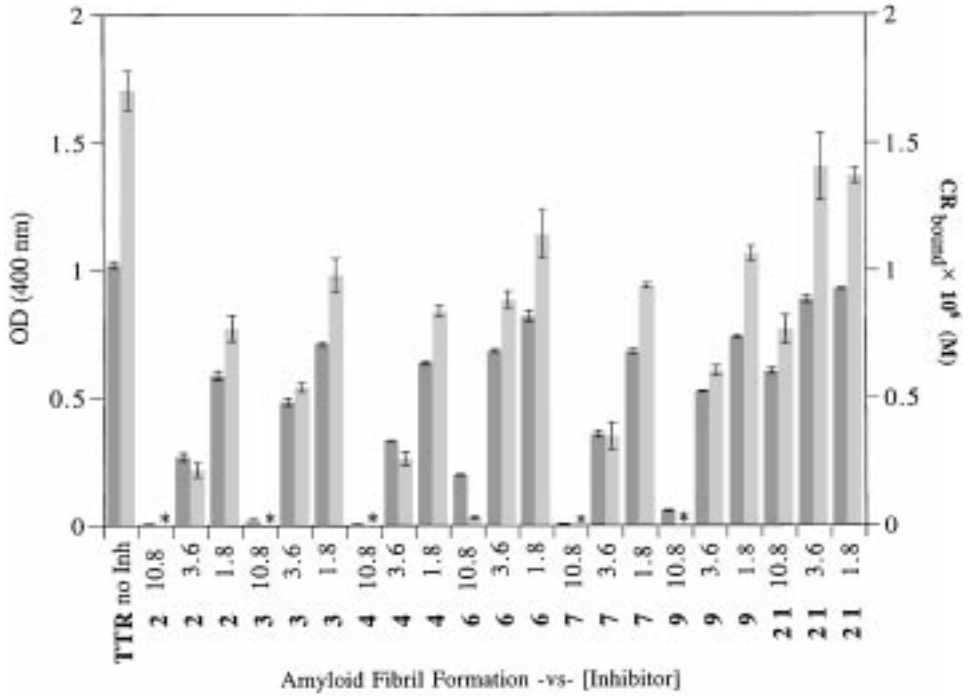

Figure 4. A bar graph representing the extent of TTR amyloid fibril formation as a function of inhibitor concentration at constant TTR concentration (3.6 μM). Dark bars represent fibril formation as evaluated by the optical density (OD) reading of the solution in a UV spectrometer at 400 nM. Lighter bars represent the extent of TTR fibril formation as evaluated by congo red binding. Each assay was done in triplicate and the error bars indicate the standard deviation. Asterisks replacing the congo red determinations indicate small negative values for congo red binding. Occasionally small negative values are observed when little or no fibril formation occurs.

of 36 μM, reflecting the greater error involved in this measurement and possibly a systematic error (Fig. 4).

Discussion

A collaboration between the Sacchettini laboratory and our own produced a 2 Å resolution crystal structure of the Flu_2·TTR complex.[19] Owing to the symmetry associated with the T_4 binding site, Flu is able to bind in two symmetry equivalent modes in each of two symmetry equivalent binding sites shown in Figure 6. In addition, Flu is able to bind in two conformations where the CF_3 group is either in a *cis* or *trans* relationship to the intramolecularly hydrogen bonded NH and COOH functional groups (Fig. 6). The crystal structure

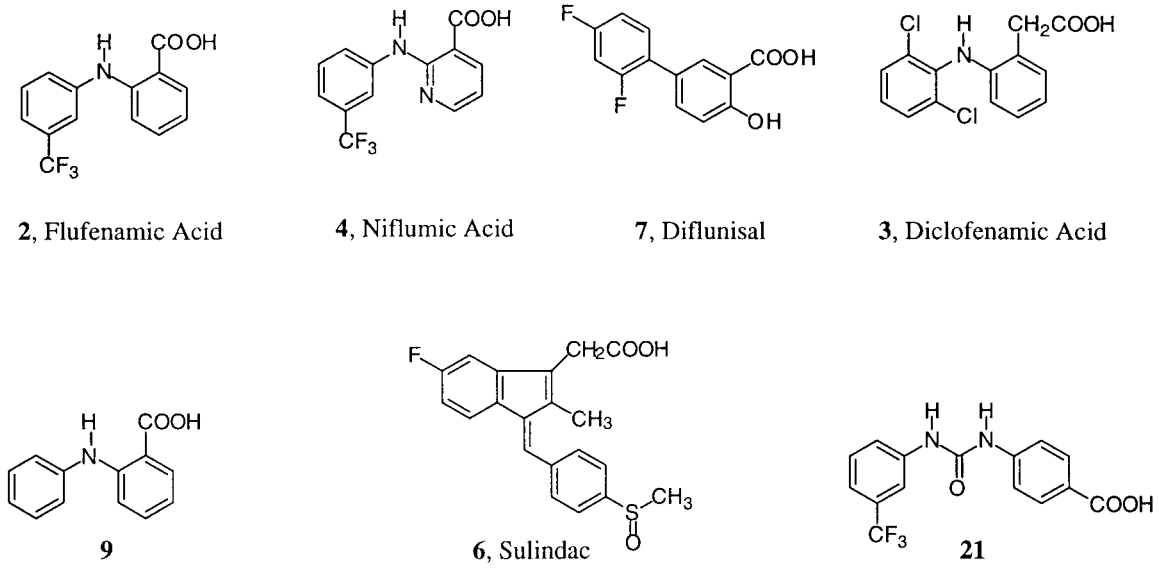

Figure 5. Structural summary of the best transthyretin amyloid fibril formation inhibitors identified in this study. The order of efficacy is: **2** > **4**≈**7** > **3** > **9** > **6** > **21**.

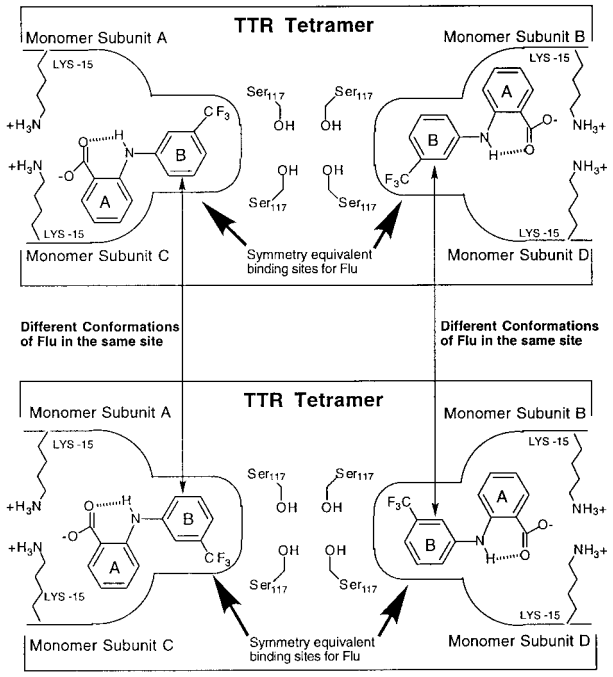

Figure 6. A schematic representation of the cocrystal structure between transthyretin and flufenamic acid. There are two symmetry equivalent flufenamic acid binding sites/tetramer, each of which can accommodate flufenamic acid in two symmetry equivalent modes. Flufenamic acid also exists in two conformations (i.e. the CF_3 substituent either being *cis* or *trans* to the intramolecular hydrogen bonded NH and COO^- groups). A more detailed description of this structure can be found in the literature.[19]

also clearly shows the interaction between the Lys-15 ammonium group from each TTR subunit and the COO^- group of Flu (Fig. 6). Interestingly, the CF_3 group of Flu is placed in a region of TTR that is quite hydrophilic in the apo structure, facilitating a structural rearrangement in TTR to accomodate the CF_3 substituent of Flu. In the apo structure, the side chains of all four Ser-117 residues are pointing towards the two T_4 binding cavities interacting with bulk H_2O filling the empty binding site. Accomodation of the CF_3 from Flu in the T_4 site causes the side chains of the Ser-117 residues on all four subunits to rotate approximately 120°, forming two non-solvated hydrogen bonds between the Ser-117 residues on adjacent subunits (four new hydrogen bonds/tetramer) (Fig. 6). These intersubunit hydrogen bonds could be important in further stabilizing the tetramer and possibly in making the off rate for inhibitor dissociation slow.

Inhibiting TTR conformational changes with small molecules is different than enzyme inhibition. Enzymes have the opportunity to rebind their inhibitors after they dissociate, whereas apo-TTR under amyloid forming conditions changes conformation and associates, denying the alternatively folded protein another chance to bind the inhibitor. The activation barrier(s) for TTR refolding are high enough to prevent the associated alternatively folded protein to be in equilibrium with folded TTR, even in the presence of high concentrations of high affinity inhibitors. That the reconstitution process has associated with it a high $\Delta G^{\ddagger}$ is reflected in the hysteresis characteristic of TTR GdnHCl mediated unfolding and reconstitution curves.[12] The other challenge associated with inhibiting the amyloidogenicity of transthyretin is its high plasma concentration (3.6 μM), necessitating high inhibitor concentrations 3.6–7.2 μM.[18]

As illustrated in Figure 1, we have segregated the structure of **2** into five groups to focus on these substructures and evaluate their importance for inhibitor efficacy. Potential inhibitors were purchased and synthesized (Figs. 2 and 3) to decipher which of the structural features of Flu (the trifluoromethyl group, the aniline nitrogen linker, the carboxylic acid group, or the diaryl system) are most important. For example, diclofenamic acid, **3**, retains the diarylamine skeleton of **2**, but has an alternative substitution pattern on the aromatic rings and possibly an altered conformation(s). Niflumic acid, **4**, is identical to Flu except for the heterocyclic aromatic ring. The remaining NSAIDs **5–8** bear less resemblance to Flu, whereas *N*-phenylanthranilic acid, **9**, is basically Flu without the trifluoromethyl group. The impressive efficacy of compound **9** as an amyloid fibril inhibitor questions the importance of the trifluoromethyl group identified in crystallographic studies as a key pharmacophore in the activity of Flu. However, a comparison of inhibitors **13** to **14** (at 10.8 μM, data not shown) and distinguishing between the inhibitor efficacy of trifluoro-substituted aryl ureas to the unsubstituted aryl ureas suggests that the CF_3 group is beneficial (Table 1 and Fig. 3). Future structural, binding and kinetic studies comparing **9** to Flu and analogous comparisons should prove particularly important for further deliniating the importance of the trifluoromethyl group.

Discovering the effectiveness of diflunisal (**7**) is arguably the most important result to come from this study. NSAID **7** is nearly equivalent to inhibitor **4** and is nearly as good as flufenamic acid (**2**) in the stagnant fibril formation assay employed in these studies. Before we can truly understand the SAR ramifications of these results with regard to Flu, a structure of the diflunisal·TTR complex and perhaps other inhibitor·TTR complexes are required, as it is likely that these aromatic compounds bind differently to TTR.

A number of compounds were synthesized varying the linker separating the two aryl rings. These linkers included the aminomethylene group in **13–15**, the urea linkers in compounds **16–27**, and the amides **28** and **29**. Incorporation of each of these linkers results in different conformational biases, separation geometries and distances relative to the substituted aryl rings. By alternating the positions of the trifluoromethyl and carboxylic acid functionalities, we were able to search a variety of conformational space in hopes of identifying combination(s) that might be best for optimizing binding of these 'linker modified' compounds to TTR. Structures **10–12** retain only a single aryl ring and were included in the bioassay portion of the experiments as controls and were inactive. The potential inhibitors **13**, **14** and **15** with the aminomethylene linker exhibit biological activity at an inhibitor concentration of 36 μM, but do

not exhibit significant biological activity at 10.8 μM concentration (data not shown). Of the urea linked compounds, only **16**, **17** and **21** showed inhibitor efficacy at a concentration of 36 μM. The remainder of the compounds mentioned in this paragraph do not exhibit impressive inhibitory properties at a concentration of 36 μM. It is tempting to speculate that the spacer (Fig. 1) is not so important, based on the observation that compounds with a variety of spacers, including a direct aryl linkage (e.g. **7**), serve as inhibitors. The ability of the TTR binding site to accomodate a number of different types of spacers is also in keeping with the results from another recent study which demonstrates that appropriately substituted stilbenes, dibenzofurans and biphenylethers are also good inhibitors.[18] Although caution is appropriate regarding drawing conclusions about the spacers as it is likely that the bound structures of these compounds with TTR will differ.

What is striking regarding the 29 compounds evaluated within is that the aromatic carboxylic acid or phenol functional group is important, but not sufficient (e.g. **12**, Fig. 3 and Table 1) for TTR fibril inhibitor efficacy. In the cocrystal structure of thyroxine·TTR, the carboxyl and amino groups of T_4 form ion pairs with Lys-15 and Glu-54 on the solvent exposed region of the binding cavity.[23,24] An ion pair is also observed between the carboxylate of flufenamic acid and the two Lys-15 ε-ammonium groups in its cocrystal structure with TTR (Fig. 6).[19] The results from these studies infer that the formation of a tight ion pair at the solvent exposed region of the binding cavity plays an important role in determining the ability of the compounds to bind to TTR. This trend was also observed in another analysis of 85 commercially available compounds.[18]

The amyloid fibril inhibitory activity of **2**, **3**, **4**, **7**, **9** and **14**, as well as the modest activity observed in several of the urea analogues (most noteably **16**, **17** and **21**) indicates that significant differences in the structural platform (aromatic template) are tolerated in the inhibitors. It is too early to be certain what the best structural platform is for a TTR amyloid fibril inhibitor. We are currently using these results as an incentive for testing a number of other commercially available and synthetically accessible compounds to identify new inhibitors or aromatic templates or both. The compounds selected for future screens will be aromatics with variable substituents containing a variety of linkers. Likely inhibitors will also contain a carboxylic acid, phenolic, or equivalent group expected to interact with one or more Lys-15 in TTR. A zwitterionic substituent will also be evaluated to interact with TTR analogously to T_4.

Conclusion

We have utilized the stagnant fibril formation assay to evaluate potential inhibitors of TTR amyloid fibril formation in vitro. Twenty nine aromatic small molecules, some with homology to flufenamic acid, were tested to identify important structural features for inhibitor efficacy. The results of these experiments and earlier screens suggest that likely inhibitors will have aromatic-based structures with at least two aromatic rings (one of the two rings can be a bi- or tricyclic aromatic ring[18]). The ring or fused ring system[18] occupying the outermost binding pocket of TTR needs to be substituted with an acidic functional group, either a phenol or carboxylic acid (Fig. 6). The promising inhibitors identified in this study ranked in order of efficacy are: **2** > **4**≈**7** > **3** > **9** > **6** > **21** (Fig. 5).

Experimental

General aspects

All glassware were oven-dried and cooled in a dessicator containing $CaSO_4$. THF was distilled from Na/benzophenone. Anhydrous methanol was obtained by distilling HPLC grade methanol from magnesium methoxide which was stored over activated 4 Å molecular sieves. Thin-layer chromatography was performed on Kodak plastic backed silica gel plates 250 μ that were visualized by UV irradiation or I_2 staining or both. Chromatographic purification on silica gel (Merck, grade 60, 240–400 mesh, 60 Å) was done by flash chromatography. ^{1}H NMR spectra were recorded at 300 or 400 MHz and ^{13}C NMR at 75 MHz using either Bruker or Varian spectrometers. A pulse delay of at least 2 s was employed to avoid losing signals for quaternary carbons. Most of the aromatic inhibitors characterized by ^{13}C NMR exhibit 7–13 resonances, slightly less that the maximal number expected ≈15, most likely due to resonance overlap. DMSO-d_6 (^{1}H δ 2.49, m, ^{13}C δ 39.5, m) or CD_3OD (^{1}H δ 4.87, s, 3.31, m; ^{13}C δ 49.15, m) were used as interal standards, coupling constants (*J*) values are reported in Hertz.

General procedure for reductive amination reactions to yield 13–15

To a round bottom flask was added the appropriate aniline (6.21 mmol), the benzaldehyde (6.21 mmol), and 2.7 mol % of acetic acid in approximately 30 mL of benzene. The solution was refluxed in a Dean–Stark apparatus for 2–24 h, the duration being dependent on the nature of the aldehyde used in the reaction. The solvent was removed by reducing the volume under reflux and then by rotary evaporation under reduced pressure. The Schiff base was dissolved in 5 mL of anhydrous methanol and cooled to 0 °C. To this stirred solution was added 0.39 g of sodium cyanoborohydride (6.21 mmol) in small portions over 5 min (vigorous bubbling was observed after the addition of solid sodium cyanoborohydride). The reaction vessel was vented to the atmosphere with a 21 gauge needle through a septa. The reaction mixture was stirred for 18 h and the methanol removed by rotary evaporation under reduced pressure. The residual material was partitioned between 50 mL of EtOAc and 5 mL of distilled H_2O and the organic layer was washed with 5 mL of brine solution before drying it over anhydrous $MgSO_4$. The solution was concentrated under vacuum and purified by either crystallization or silica gel chromatography.

Summary of spectral data

13: ^{1}H NMR (300 MHz, DMSO-d_6): δ 7.96 (d, J= 7.9 Hz, 2H), 7.5 (d, J=7.9 Hz, 2H), 7.25 (dd, J=8, 7.8 Hz), 6.85 (m, 4H, including ArH and NH), 4.43 (d, J=3.9 Hz, 2H); ^{13}C NMR (75 MHz, CD_3OD): δ 150.38, 146.72, 131.17, 130.80, 128.26, 116.79, 113.884, 109.96, 48.04 HRMS (FAB) calcd for $C_{15}H_{12}F_3NO_2$ 296.0898, found 296.0897 $(M+H)^+$.

14: ^{1}H NMR (300 MHz, CD_3OD): δ 7.73 (d, J= 8.84 Hz, 2H), 7.45–7.35 (m, 5H), 6.57 (d, J=8.84 Hz, 2H), 4.36 (s, 2H); ^{13}C NMR (75 MHz, CD_3OD): δ 155.5, 132.74, 129.64, 128.32, 128.11, 1112.55, 47.89; HRMS (FAB) calcd for $C_{14}H_{13}NO_2$ 228.1025, found 228.1024 $(M+H)^+$.

15: ^{1}H NMR (300 MHz, DMSO-d_6): δ 7.94 (d, J=7.8 Hz, 2H), 7.48 (d, J=8.1 Hz, 2H), 7.35 (t, J=5.6 Hz, 1H), 7.13 (s, 2H), 7.15 (s, 1H); ^{13}C NMR (75 MHz, CD_3OD): δ 151.14, 145.51, 133.66, 133.23, 131.26, 128.26, 112.84, 109.74, 47.78; HRMS (FAB) calcd for $C_{16}H_{11}F_6NO_2$ 364.0772, found 364.0779 $(M+H)^+$.

General procedure for urea formation reactions to afford 16–27

A round-bottom flask was charged with the appropriate aniline in 5 mL of anhydrous THF under N_2. The solution was cooled to 0 °C and the appropriate isocyanate was added dropwise over 30 s. The reaction was allowed to warm to room temperature. In general, a heavy precipitate forms within 5–60 min. In the case of the more sterically constrained systems bearing *ortho* substituents, the reaction may require up to 24 h to precipitate. The products were collected by vacuum filtration and the solids washed with 25–50 mL of dichloromethane before drying the urea under vacuum.

Summary of spectral data

16: ^{1}H NMR (300 MHz, DMSO-d_6): δ 10.31 (s, 1H), 9.19 (s, 1H), 8.26 (d, J=8.64 Hz, 1H), 7.85 (d, J= 8.12 Hz, 1H), 7.61 (d, J=7.84 Hz, 1H), 7.54 (dd, 2H), 7.41 (dd, J=7.6 Hz, 1H), 7.3 (dd, J=6.5 Hz, 1H), 6.93 (dd, J=7.48 Hz, 1H); ^{13}C NMR (75 MHz, DMSO-d_6): δ 169.45, 153.66, 142.15, 136.07, 133.78, 133.11, 131.12, 130.11, 126.46, 126.41, 126.13, 121.25. 120.26, 116.21; HRMS (FAB) calcd for $C_{15}H_{11}F_3N_2O_3$ 325.0800, found 325.0804 $(M+H)^+$.

17: ^{1}H NMR (300 MHz, DMSO-d_6): δ 9.61 (s, 1H), 8.17 (dd, J=1.88 Hz, 1H), 8.08 (s, 1H), 7.96 (d, J=8.08 Hz, 1H), 7.65 (m, 4H), 7.40 (dd, J=8.12, 7.84 Hz, 1H), 7.24 (dd, J=7.56 Hz, 1H); ^{13}C NMR (75 MHz, DMSO-d_6): δ 167.39, 152.58, 139.89, 136.30, 132.98, 131.56, 129.24, 126.04, 125.92, 125.81, 123.88, 123.09, 122.36, 118.96; HRMS (FAB) calcd for $C_{15}H_{11}F_3N_2O_3$ 325.0800, found 325.0803 $(M+H)^+$.

18: ^{1}H NMR (300 MHz, DMSO-d_6): δ 9.72 (s, 1H), 8.19 (s, 1H), 7.93 (m, 3H), 7.6 (m, 4H), 7.23 (dd, J=7.32, 7.56 Hz, 1H); ^{13}C NMR (75 MHz, DMSO-d_6): δ 167.40, 152.55, 144.06, 136.27, 133.02, 130.93, 126.12, 124.30, 124.09, 117.57; HRMS (FAB) calcd for $C_{15}H_{11}F_3N_2O_3$ 325.0800, found 325.0804 $(M+H)^+$.

19: ^{1}H NMR (300 MHz, DMSO-d_6): δ 10.53 (s, 1H), 10.18 (s, 1H), 8.41 (d, J=8.44 Hz, 1H), 8.04 (s, 1H), 7.23 (d, J=8.08 Hz, 1H), 7.72 (d, J=8.84 Hz, 1H), 7.50 (dd, dd, J=7.36, 9.2, 8.44, 8.08 Hz, 2H), 7.25 (d, J=7.72 Hz, 1H), 7.03 (dd, J=7.72, 7.36 Hz, 1H); ^{13}C NMR (75 MHz, DMSO-d_6): δ 169.71, 152.38, 142.13, 140.85, 133.92, 131.18, 129.89, 122.13, 121.27, 119.96, 188.34, 116.46, 115.67, 114.67; HRMS (FAB) calcd for $C_{15}H_{11}F_3N_2O_3$ 325.0800, found 325.0804 $(M+H)^+$.

20: ^{1}H NMR (300 MHz, DMSO-d_6): δ 9.06 (s, 1H), 9.01 (s, 1H), 8.20 (s, 1H), 8.04 (s, 1H), 7.66 (d, J=8.0 Hz, 1H), 7.59 (d, J=5.12 Hz, 1H), 7.58 (d, J=4.6 Hz, 1H), 7.45 (dd, J=7.56, 8.08 Hz, 1H), 7.38 (dd, J=7.84, 8.08 Hz, 1H), 7.25 (d, J=7.0 Hz, 1H); ^{13}C NMR (75 MHz, DMSO-d_6): δ 167.77, 152.95, 140.88, 140.10, 131.82, 130.14, 129.38, 123.44, 123.06, 122.28, 119.62, 118.51, 114.72; HRMS (FAB) calcd for $C_{15}H_{11}F_3N_2O_3$ 325.0800, found 325.0805 $(M+H)^+$.

21: ^{1}H NMR (300 MHz, DMSO-d_6): δ 9.14 (s, 1H), 9.12 (s, 1H), 8.01 (s, 1H), 7.89 (d, J=8.64 Hz, 2H), 7.59 (d, J=8.64 Hz, 2H), 7.56 (s, 1H), 7.46 (dd, J=7.48 Hz, 1H), 7.26 (d, J=7.56 Hz, 1H); ^{13}C NMR (75 MHz, DMSO-d_6): δ 167.59, 152.61, 144.06, 140.59, 130.95, 130.05, 129.90, 124.41, 122.26, 118.65, 117.87, 114.78; HRMS (FAB) calcd for $C_{15}H_{11}F_3N_2O_3$ 325.0800, found 325.0804 $(M+H)^+$.

22: ^{1}H NMR (300 MHz, DMSO-d_6): δ 10.54 (s, 1H), 10.22 (s, 1H), 8.41 (d, J=7.72 Hz, 1H),), 7.97 (d, J= 7.9 Hz, 1H), 7.75 (d, J=8.46 Hz, 2H), 7.59 (d, J= 8.82 Hz, 2H), 7.51 (dd, J=7.72, 7.54 Hz, 1H), 7.02 (dd, J=7.88, 7.74 Hz, 1H); ^{13}C NMR (75 MHz, DMSO-d_6): δ 169.74, 152.32, 143.79, 142.15, 133.89, 131.22, 126.08, 126.05, 121.31, 120.09, 118.44, 115.84; HRMS (FAB) calcd for $C_{15}H_{11}F_3N_2O_3$ 325.0800, found 325.0806 $(M+H)^+$.

23: ^{1}H NMR (300 MHz, DMSO-d_6): δ 9.09 (s, 1H), 9.0 (s, 1H), 8.20 (s, 1H), 7.70–7.55 (6d/m, 6H), 7.38 (dd, J=7.84 Hz, 1H); ^{13}C NMR (75 MHz, DMSO-d_6): δ 167.60, 152.55, 143.55, 139.87, 131.67, 129.16, 126.21, 126.16, 123.32, 122.84, 119.44, 118.18; HRMS (FAB) calcd for $C_{15}H_{11}F_3N_2O_3$ 325.0800, found 325.0804 $(M+H)^+$.

24: ^{1}H NMR (300 MHz, DMSO-d_6): δ 9.17 (s, 1H), 9.14 (s, 1H), 7.93 (dd, J=8.64 Hz, 2H),), 7.67 (dd, J= 8.36 Hz, 2H), 7.59 (m, 4H); ^{13}C NMR (75 MHz, DMSO-d_6): δ 167.42, 152.28, 143.90, 143.37, 130.85, 126.26, 126.22, 124.33, 118.25, 117.69; HRMS (FAB) calcd for $C_{15}H_{11}F_3N_2O_3$ 325.0800, found 325.0803 $(M+H)^+$.

25: ^{1}H NMR (300 MHz, DMSO-d_6): δ 10.45 (s, 1H), 9.83 (s, 1H), 8.43 (d, J=8.64 Hz, 1H),), 7.99 (d, J= 7.8 Hz, 1H), 7.59 (d, J=7.84 Hz, 2H), 7.57 (dd,

$J = 7.8$ Hz, 2H), 6.95 (dd, dd, $J = 7.84$ Hz, 2H); ^{13}C NMR (75 MHz, DMSO-d_6): δ 169.73, 152.55, 142.54, 139.96, 133.89, 131.21, 128.87, 122.29, 120.99, 120.08, 119.03; HRMS (FAB) calcd for $C_{14}H_{12}N_2O_3$ 257.0848, found 257.0851 $(M+H)^+$.

26: ^{1}H NMR (300 MHz, DMSO-d_6): δ 8.9 (s, 1H), 8.69 (s, 1H), 8.19 (dd, $J = 1.88$ Hz, 1H), 7.69 (d, $J = 7.82$ Hz, 1H), 7.59 (d, $J = 7.84$ Hz, 1H), 7.45 (d, $J = 7.8$ Hz, 2H), 7.39 (dd, $J = 7.82$ Hz, 1H), 7.25 (dd, $J = 7.85$ Hz, 2H), 6.98 (dd, $J = 6.2$ Hz, 1H); ^{13}C NMR (75 MHz, DMSO-d_6): δ 167.58, 152.73, 140.19, 139.74, 131.56, 129.17, 128.97, 122.93, 122.58, 122.18, 119.12, 118.57; HRMS (FAB) calcd for $C_{14}H_{12}N_2O_3$ 257.0848, found 257.0850 $(M+H)^+$.

27: ^{1}H NMR (300 MHz, DMSO-d_6): δ 9.04 (s, 1H), 8.76 (s, 1H), 7.98 (d, $J = 8.36$ Hz, 2H), 7.65 (d, $J = 8.36$ Hz, 2H), 7.51 (d, $J = 7.8$ Hz, 2H), 7.26 (dd, $J = 7.56$, 7.28 Hz, 2H), 6.94 (dd, $J = 7.04$ Hz, 1H); ^{13}C NMR (75 MHz, DMSO-d_6): δ 167.72, 152.72, 144.49, 139.76, 131.85, 129.22, 124.16, 122.62, 118.93, 117.71; HRMS (FAB) calcd for $C_{14}H_{12}N_2O_3$ 257.0921, found 257.0926 $(M+H)^+$.

General procedure for benzamide forming reactions to afford 28 and 29

A round-bottom flask was charged with the appropriate aniline (7.3 mmol) in 5 mL of anhydrous THF under N_2. The solution was cooled to 0 °C and *meta*-trifluoromethylbenzoyl chloride (3.3 mmol) was added dropwise over 30 s. The reaction was allowed to warm to room temperature. After 24 h, the solution was partitioned between 50 mL EtOAc and 40 mL of 1 N HCl. The organic layer was washed with H_2O and brine, dried over anhydrous $MgSO_4$, and concentrated under reduced pressure. The resulting solids were crystallized from MeOH:EtOAc:hexanes.

Summary of spectral data

28: ^{1}H NMR (300 MHz, DMSO-d_6): δ 8.43 (dd, $J = 1.88$ Hz, 1H), 8.33 (s, 1H), 8.28 (d, $J = 7.84$ Hz, 1H), 8.08 (d, $J = 7$ Hz, 1H), 7.91 (d, $J = 7.84$ Hz, 1H), 7.72 (dd, $J = 7.84$ Hz, 2H), 7.47 (dd, $J = 8.08$, 7.84 Hz, 1H); ^{13}C NMR (75 MHz, CD_3OD): δ 167.35, 164.28, 139.24, 135.59, 132.02, 131.41, 129.79, 129.05, 128.34, 124.92, 124.66, 124.47, 124.43 121.44; HRMS (FAB) calcd for $C_{15}H_{10}F_3NO_3$ 310.0691, found 310.0687 $(M+H)^+$.

29: ^{1}H NMR (300 MHz, DMSO-d_6): δ 8.29 (s, 1H), 8.26 (d, $J = 8.08$ Hz, 1H), 7.93 (m, 5H), 7.78 (dd, $J = 7.84$ Hz, 1H); ^{13}C NMR (75 MHz, CD_3OD): δ 166.96, 164.54, 142.98, 132.06, 130.34, 129.85, 128.44, 125.86, 124.47, 119.74, 119.65; HRMS (FAB) calcd for $C_{15}H_{10}F_3NO_3$ 310.0691, found 310.0688 $(M+H)^+$.

Three day stagnant fibril forming assay

The compounds were tested by following the previously published protocol incorporating the following changes.[4] The compounds were originally prepared as 5.4 mM solutions in pure DMSO such that only 2 μL of solution was required to reach the desired concentration (36 μM, 10× TTR concentration) in a 300 μL assay. In the case of the lower concentrations of inhibitors (10.8 μM, 3.6 μM TTR, 1.8 μM), serial dilutions were made of the 36 μM inhibitor solutions such that 2 μL provided the desired amount of compound to be tested. All of the compounds were prepared by weighing a known amount of material and making the appropriate addition of DMSO. The remainder of the assay was performed as described, except for inhibitors that absorbed at 330 nM, in which case 400 nM light was employed for the optical density measurements.

Acknowledgements

We thank the National Institutes of Health (NIH R01 DK46335), the Lita Annenberg Hazen Family, the Skaggs Family, and the NIH-NRSA to P.B. (F32 GM18451-01) for partial funding of this work.

References

1. Kelly, J. W. *Curr. Op. Struct. Biol.* **1996**, *6*, 11.
2. Kelly, J. W. *Structure* **1997**, *5*, 595.
3. Kelly, J. W. *Curr. Op. Struct. Biol.* **1998**, *8*, 101.
4. Lansbury, P. T. *Biochemistry* **1992**, *31*, 6865.
5. Sipe, J. D. *Ann. Rev. Biochem.* **1992**, *61*, 947.
6. Sipe, J. D. *Crit. Rev. in Clin. Lab. Sci.* **1994**, *31*, 325.
7. Jacobson, D. R.; Buxbaum, J. N. *Adv. Hum. Genet.* **1991**, *20*, 69.
8. Benson, M. D. *TIBS* **1989**, *12*, 88.
9. Colon, W.; Kelly, J. W. *Biochemistry* **1992**, *31*, 8654.
10. Kelly, J. W.; Lansbury, P. T. J. *Amyloid: Int. J. Exp. Clin. Invest.* **1994**, *1*, 186.
11. Lai, Z.; Colon, W.; Kelly, J. W. *Biochemistry* **1996**, *35*, 6470.
12. Lai, Z.; McCulloch, J.; Kelly, J. W. *Biochemistry* **1997**, *36*, 10230.
13. McCutchen, S.; Colon, W.; Kelly, J. W. *Biochemistry* **1993**, *32*, 12119.
14. McCutchen, S. L.; Lai, Z.; Miroy, G.; Kelly, J. W.; Colon, W. *Biochemistry* **1995**, *34*, 13527.
15. Miroy, G. J.; Lai, Z.; Lashuel, H.; Peterson, S. A.; Strang, C.; Kelly, J. W. *Proc. Natl. Acad. Sci. USA* **1996**, 93, 15051.
16. Lashuel, H. A.; Lai, Z.; Kelly, J. W. *Biochemistry* **1998**, *37*, 17851.
17. Inlow, J.; Lai, V.; Kelly, J. W. *Biochemistry* **1998**, *37*, in press.
18. Baures, P. W.; Peterson, S. A.; Kelly, J. W. *Bioorg. Med. Chem. Lett.* **1998**, *6*, 1389.
19. Peterson, S. A.; Klabunde, T.; Lashuel, H. A.; Purkey, H.; Sacchettini, J. C.; Kelly, J. W. *Proc. Natl. Acad. Sci. USA* **1998**, *95*, 12956.
20. Borch, R. F.; Bernstein, M. D.; Durst, H. D. *J. Am. Chem. Soc.* **1971**, *93*, 2897.
21. Satchell, D. P. N.; Satchell, R. S. *Chem. Soc. Rev.* **1975**, *4*, 231.
22. Klunk, W. E.; Pettegrew, J. W.; Abraham, D. J. *J. Histochem. Cytochem.* **1989**, *37*, 1273.
23. Wojtczak, A.; Luft, J.; Cody, V. *J. Biol. Chem.* **1992**, *267*, 353.
24. Wojtczak, A.; Cody, V.; Luft, J. R.; Pangborn, W. *Acta Cryst.* **1996**, *D52*, 758.